Available online at www.eccomasproceedia.org
Eccomas Proceedia COMPDYN (2023) 2335-2347

ECCOMAS
Proceedia

COMPDYN 2023
9th ECCOMAS Thematic Conference on
Computational Methods in Structural Dynamics and Earthquake Engineering
M. Papadrakakis, M. Fragiadakis (eds.)
Athens, Greece, 12-14 June 2023

BAYESIAN UPDATING OF WOODEN STRUCTURAL PARAMETERS AND SEISMIC DAMAGE CLASSIFIER USING NEURAL NETWORK

Rikuto Mizobuchi[1], **Masayuki Kohiyama**[1], **and Takuzo Yamashita**[2]

[1] School of Science and Technology, Keio University
3-14-1 Hiyoshi, Kohoku-ku, Yokohama, Kanagawa, 223-8522, Japan
rikuto.mizobuchi@keio.jp, kohiyama@sd.keio.ac.jp

[2] National Research Institute for Earth Science and Disaster Resilience
3-1 Tennodai, Tsukuba, Ibaraki, 305-0006, Japan
tyamashi@bosai.go.jp

Abstract

Structural health monitoring is an effective way to quickly and efficiently detect earthquake damage to a building. However, its applications to wooden buildings are still limited. One of the challenges in predicting the seismic response of a wooden structure is that the effect of variance in its material and structural properties is relatively significant. To handle this problem, we propose a method to update the damage classifier using Bayesian system identification. The damage classifier is constructed using neural network (NN) and machine learning techniques. The method utilizes the weighted loss function for the NN to reflect the updated probability distribution of the structural parameters. The NN is tuned using backpropagation, where the training data are consequently weighed by the weighed loss function, directly using the value of the posterior probability, according to the data obtained from the numerical model of a target structure with the corresponding parameters. Using the result of the Bayesian updating, the tuned NN damage classifier achieved a higher accuracy than before tuning by reflecting the posterior probability distribution of the structural parameters.

Keywords: Structural Health Monitoring, Bayesian Updating, Deep Neural Network, Wooden Structure.

doi: 10.7712/120123.10564.20678

1 INTRODUCTION

Prompt assessment of structural damage after an earthquake is extremely important to prevent secondary disasters that may affect human lives, such as collapse due to aftershocks. The current method in Japan, called Post-earthquake Quick Inspections, is conducted by volunteer experts with architectural knowledge, putting up a tag on the wall of an assessed building that is either green, yellow, or red, depending on the degree of damage. However, there are concerns that the safety of the inspectors cannot be guaranteed, and that the number of inspectors may not be sufficient to quickly assess numerous buildings in the event of a large-scale earthquake.

In the 2016 Kumamoto earthquakes, two large earthquakes occurred within a short period of time, and many wooden house collapses were reported [1]. In the case of consecutive strong earthquake motions within a short time, the residents who evacuated after the first strong earthquake motion, may return to their homes unaware of the danger posed by buildings. In such cases, the current inspection system may not be able to avert the danger in timely manner.

Based on the above case, a structural health monitoring (SHM) system for wooden structures is expected to be developed for rapid and automatic detection of earthquake-induced damage, using observation records from sensor networks. SHM systems are currently mainly applied to large-scale civil structures and their application to low-rise buildings such as wooden houses is still limited.

Peterson et al. [2] verified the validity of single member damage identification in wooden structures by performing finite element analysis and impact experiments on wooden beams, and they were able to identify the location of damage. In addition, methods for identifying damage not only to individual members but also to the full wooden building have also been studied. Nakamura et al. [3] proposed a method to detect damage based on changes in natural frequencies before and after an earthquake, and Shiomitsu and Sakai [4] proposed a method to detect damage based on changes in natural period using acceleration sensors.

The neural network (NN) is a machine learning-based method that can be used as a damage detection method in SHM systems. Tanida et al. [5] used three-layer and four-layer NNs to discriminate damaged areas in a wooden frame model.

One of the challenges in predicting the seismic response of a wooden structure is that the effect of variance in its material and structural properties is relatively significant. When modelling existing structures for seismic response analysis, the uncertainty in their parameters cannot be ignored. The objective of this study was to refine the distribution of structural parameters using Bayesian updating and to improve the accuracy of discriminating the collapse hazard of wooden structures using NNs.

2 CONSTRUCTION OF NEURAL NETWORK DAMAGE CLASSIFIER

2.1 Overview of proposed methodology

We propose an SHM system to classify the collapse risk of wooden structures induced by *second* strong earthquake. The system considers two phases: construction and operation; the workflow of these phases is shown in **Fig. 1**. In the construction phase, the numerical model of the target structure is first built to perform time-history response analysis. The model is duplicated with varying values of structural parameters to account for the uncertainty in material and structural properties. Seismic response analysis is performed to the prepared model with various input seismic motions to generate a large amount of simulated structural response data. Then, the second seismic motion is subjected to the model to evaluate the remaining performance to classify the collapse risk induced by the second strong earthquake. The NN damage classifier is trained using the dataset from the response data of the first simulation, and the classification label of the remaining performance of the model.

In the operational phase of the method, it is assumed that the building will experience small- to medium-scale earthquake ground motion prior to large-scale earthquake ground motion. The response data of the small- to medium-scale earthquake ground motion is used to refine the probability distribution of structural parameters.

After monitoring the structural response of the small- to medium-scale earthquake ground motion, another seismic response analysis is performed by inputting the observed ground motion to the numerical model. By comparing the measured and simulated responses, Bayesian updating is performed to derive the posterior distribution of structural parameters. The value of the posterior distribution is used to update the NN damage classifier.

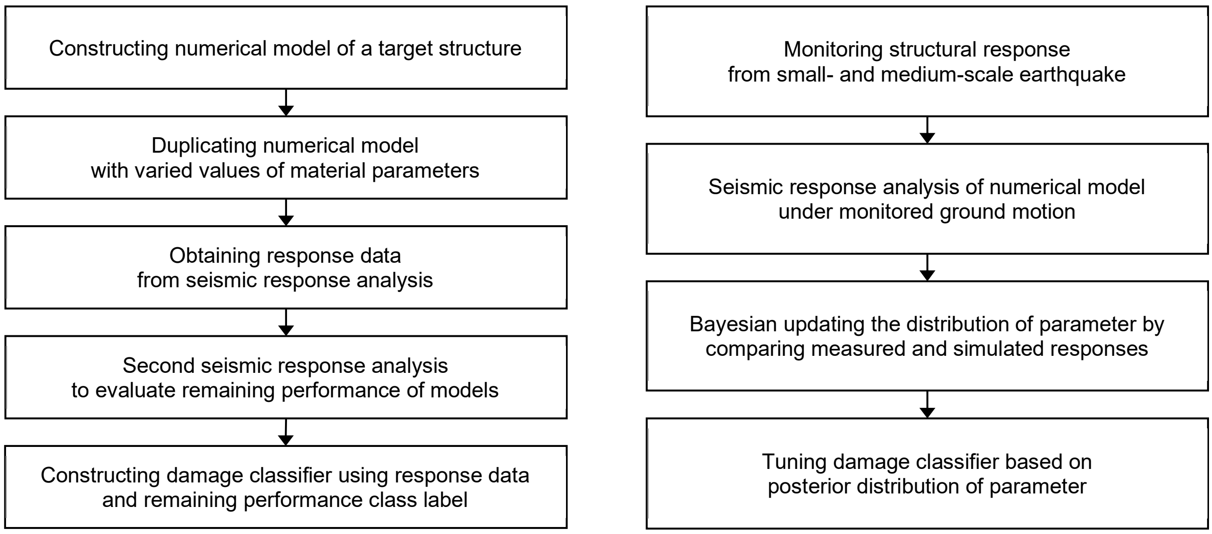

(a) Construction phase (b) Operational phase

Figure 1: Workflow of the proposed method.

2.2 Bayesian updating

Suppose that a dataset $\mathcal{D} = \{u,\ \boldsymbol{q}\}$ is available, consisting of output $\boldsymbol{q}$ of the system, corresponding the system input u. The probability model $p(\boldsymbol{q}|u, \boldsymbol{\theta}, \mathcal{M})$ in the set defined by model $\mathcal{M}$ can be quantified by the posterior probability distribution function (PDF) $p(\boldsymbol{\theta}|\mathcal{D}, \mathcal{M})$ for the uncertain model parameters $\boldsymbol{\theta}$ which specify a particular model within $\mathcal{M}$ [6]. Using Bayes' Theorem:

$$p(\boldsymbol{\theta}|\mathcal{D}, \mathcal{M}) = \frac{p(\mathcal{D}|\boldsymbol{\theta}, \mathcal{M})p(\boldsymbol{\theta}|\mathcal{M})}{p(\mathcal{D}|\mathcal{M})} \tag{1}$$

where $p(\mathcal{D}|\mathcal{M}) = \int p(\mathcal{D}|\boldsymbol{\theta}, \mathcal{M})p(\boldsymbol{\theta}|\mathcal{M})\, d\boldsymbol{\theta}$ is the normalizing constant, or the evidence; $p(\mathcal{D}|\boldsymbol{\theta}, \mathcal{M})$ is the likelihood function, which expresses the probability of getting data $\mathcal{D}$ based on the PDF $p(\boldsymbol{q}|u, \boldsymbol{\theta}, \mathcal{M})$ for the system output given by the model $\mathcal{M}$; and $p(\boldsymbol{\theta}|\mathcal{M})$ is the prior PDF specified by $\mathcal{M}$ which is chosen to quantify the initial plausibility of each model defined by the value of the parameter vector $\boldsymbol{\theta}$.

The predictive PDF for the system output $\boldsymbol{q}_i \in \mathbb{R}^{N_o}$ at discrete time i ($i = 1, \dots, N_t$), conditional on the parameter vector $\boldsymbol{\theta}$, is given by the following Gaussian PDF with the mean equal to the output $\boldsymbol{q}_i(u, \boldsymbol{\theta})$ and with covariance matrix of the simulation error $\boldsymbol{\Sigma} \in \mathbb{R}^{N_o \times N_o}$:

$$p(\mathcal{D}|\boldsymbol{\theta},\mathcal{M}) = \prod_{i=1}^{N_t} \frac{1}{(2\pi)^{N_o/2}|\boldsymbol{\Sigma}|^{1/2}} \exp\left[-\frac{1}{2}\left(\boldsymbol{q}_i - \widehat{\boldsymbol{q}}_i(\boldsymbol{\theta})\right)^{\mathrm{T}}\boldsymbol{\Sigma}^{-1}\left(\boldsymbol{q}_i - \widehat{\boldsymbol{q}}_i(\boldsymbol{\theta})\right)\right] \tag{2}$$

$$\boldsymbol{\Sigma} = \begin{bmatrix} \sigma_1^2 & & 0 \\ & \ddots & \\ 0 & & \sigma_{N_o}^2 \end{bmatrix}, \qquad \sigma_j^2 = \sum_t \frac{1}{N_t}\left(q_j(t) - \hat{q}_j(t)\right)^2 \; (j = 1, \dots, N_o) \tag{3}$$

where N_o is the number of measurement channels, $\boldsymbol{q}_i$ is the measured output data, and $\widehat{\boldsymbol{q}}_i$ is the output data from simulation with model parameter $\boldsymbol{\theta}$ [6,7].

The likelihood function typically reaches very large values; thus the natural logarithm of the likelihood function is used to avoid numerical overflow [8, 9], which is expressed as follows:

$$\begin{aligned} J(\mathcal{D}|\boldsymbol{\theta},\mathcal{M}) &= \ln p(\mathcal{D}|\boldsymbol{\theta},\mathcal{M}) \\ &= -\frac{N_t N_o}{2}\ln 2\pi - \frac{N_t N_o}{2}\ln|\boldsymbol{\Sigma}| - \sum_{i=1}^{N_t}\left\{\frac{1}{2}\left(\boldsymbol{q}_i - \widehat{\boldsymbol{q}}_i(\boldsymbol{\theta})\right)^{\mathrm{T}}\boldsymbol{\Sigma}^{-1}\left(\boldsymbol{q}_i - \widehat{\boldsymbol{q}}_i(\boldsymbol{\theta})\right)\right\} \end{aligned} \tag{4}$$

2.3 Constructing neural network damage classifier

For the dataset used to train the NN, the acceleration response time-history data are used as the input data, and the classification label is used as output data. The dataset used to train the NN damage classifier is randomly selected from the total data, dividing them in an 8:2 ratio for training and validation.

The sample time length of the input time-history data is set to 1 s so that at least one history loop could be drawn, taking into account the first natural period of the target building. The number of elements of the input data is determined by (number of acceleration sensors) × (number of directional components) × (sampling frequency) × (duration of time segment).

According to the Ministry of Construction Notification No. 1457, May 31, 2000, the ratio of the safety limit displacement of a wooden building to the height of each floor (referred to as inter-story drift angle) is defined as 1/30 rad. In the proposed method, if the maximum inter-story drift angle experienced during the simulated second strong earthquake is greater than 1/30 rad, it is labelled as having a risk of collapse (class label 1); otherwise, it is labelled as having no risk (class label 0). Therefore, the damage classifier gives a binary classification to determine whether or not there is a risk of collapse. If the value of the output of the damage classifier is greater than or equal to 0.5, it determines the class as 1, and if the value is less than 0.5, it determines the class as 0.

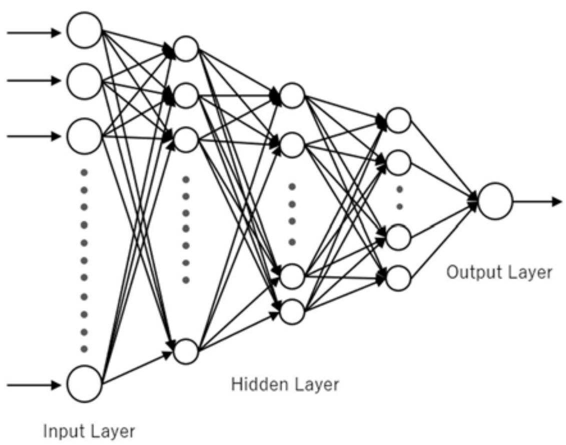

Figure 2: Deep neural network.

The NN damage classifier in this study was constructed with reference to the damage detection artificial intelligence system developed by the National Research Institute for Earth Science and Disaster Prevention (NIED) and Mizuho Information & Research Institute [10]. The NN consists of one input, one output, and three hidden layers—five layers in total—as shown in **Fig. 2**.

The output layer uses binary cross-entropy error as the loss function and sigmoid function as the activation function for binary classification of damage states. Cross-entropy is a theory used to calculate the learning error, especially when dealing with NN-based classification problems.

$$L_{\mathrm{BCE}}(t,y) = -\sum_{n=1}^{N}\{t_n \log y_n + (1-t_n)\log(1-y_n)\} \tag{5}$$

$$y = \frac{1}{1+\mathrm{e}^{-u}} \tag{6}$$

N is the total number of data, t is the label of the training data, which is the target value, u is the value stored in the nodes of the output layer, and y is the output. The term $(1-t_n)\log(1-y_n)$ penalizes false positives as it is zero when the prediction is correct.

The parameters are updated so that the loss function is minimized. The output labels obtained from the sigmoid function can be treated as the classification probability of damage.

2.4 Tuning neural network from posterior distribution

The use of weighted cross entropy loss is known in classification for unbalanced data. In the basic form of cross entropy, all data are treated equally; hence, classes with few samples tend to be ignored because they do not contribute significantly to the total loss. An effective way to remedy this problem is to assign suitable weights to each class represented in the following equation.

$$L_{\mathrm{W}}(t_i,y_i) = -w_i \cdot L(t_i,y_i) \tag{7}$$

where w is a weight vector whose value can be user-chosen. The larger the value of w, the higher the importance of the specified class during training.

In this paper we propose a custom weighted cross entropy using the posterior distribution earned from the Bayesian updating. When the numerical model $\mathcal{M}$ with parameter $\boldsymbol{\theta}_{\mathrm{k}}$ is defined as $M_k(k=1,\dots,N_M)$, the posterior distribution can be written as $p(M_k|\mathcal{D},\mathcal{M})$. By applying the values of the posterior distribution as w, corresponding to the data in model M_k, the importance of the model parameter $\boldsymbol{\theta}_{\mathrm{k}}$ can be specified. The weighted binary cross entropy can be writtten as follows:

$$L_{\mathrm{WBCE}}(t,y) = -\sum_{k=1}^{N_M}\left\{p(M_k|\mathcal{D},\mathcal{M})\cdot\frac{1}{N_k}\sum_{n\in D_k}\{-t_n\log y_n-(1-t_n)\log(1-y_n)\}\right\} \tag{8}$$

D_k is the dataset corresponding to model M_k, which includes N_k data.

3 VALIDATING THE EFFECTIVENESS OF THE PROPOSED METHOD

3.1 Target building

In this study, we set the target building based on shaking table experiments of a full-scale three-story wooden building test-specimen No. 4 from the project entitled "Experiments on Verification of Design Methods for 3-Story Wooden Frame Construction" conducted by E-

Defense of the National Research Institute for Earth Science and Disaster Resilience [11]. We created the numerical model of the specimen and performed three-dimensional structural response analyses using *wallstat* [12], a numerical analysis software for a wooden structure. The analysis software uses the discrete element method, a non-continuum analysis method developed by Nakagawa [12], as the basic theory. This enables the simulation of the collapse behavior of wooden houses, which has been difficult in the past. **Figure 3** shows an overall view of the full-scale specimen in the shaking table experiment and the numerical model generated by *wallstat*.

Figure 3: Photo of the full-scale specimen in the shaking table experiment [11] and the numerical model.

A total of four acceleration sensors are located in the center of each floor and on the roof. The maximum inter-story drift angle $\theta_{\max}$ used in this study is the maximum with respect to both time and the four corners of the first floor of the building:

$$\begin{gathered} \theta_{i\_\max} = \max(|\delta_i|/H) \\ \theta_{\max} = \max\left(\theta_{\mathrm{C1\_max}}, \theta_{\mathrm{C2\_max}}, \theta_{\mathrm{C3\_max}}, \theta_{\mathrm{C4\_max}}\right) \end{gathered} \tag{9}$$

where δ_i is the inter-story drift of the first story, and H = 2.8 m is the floor height in this specimen.

3.2 Material parameters

The variation of the parameters of each member is determined from the results of the experimental data of the members [11], which are conducted together with the shaking table experiments. In this study, two types of walls were considered as the parameters with uncertainty. The skeleton curve of the two types of walls from the member experiments are shown in **Fig. 4**.

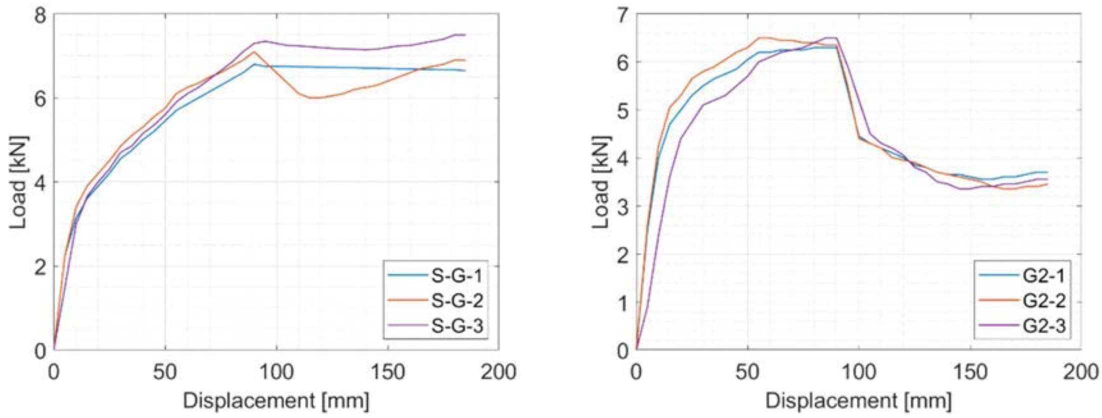

Figure 4: Skeleton curves of two types of walls obtained from member experiments.

Using the average values of the skeleton curves obtained in **Fig. 4**, the values of the yield strength are obtained by the following method.

1. Draw "line I" connecting two points on the envelope curve at $0.1P_{\max}$ and $0.4P_{\max}$.
2. Draw "line II" connecting two points on the envelope curve at $0.4P_{\max}$ and $0.9P_{\max}$.
3. Draw "line III" parallel to "line II" so that it is tangent to the envelope curve.
4. Define the load at the intersection of "line I" and "line III" as the yield capacity P_y. Draw "line IV" from P_y, parallel to the *x*-axis.
5. Define the displacement at the intersection of "line IV" and the envelope curve as the yield displacement δ_y.

We assume that the distribution of variation in yield strength follows a lognormal distribution. The mean and standard deviation of P_y in two walls are given in **Table 1**.

Member	Parameter	Mean [kN]	SD [kN]
Wall (S-G)	Yield strength P_y	3.60	0.151
Wall (G2)	Yield strength P_y	4.07	0.126

Table 1: Variation of wall parameters.

Using the following equation, the probability density of the parameter is discretized so that the area is divided into three equal parts.

$$R_i = 3 \cdot \int_{P_{y_{(i-1)/3}}}^{P_{y_{i/3}}} P_y \cdot f(P_y)\, dP_y \tag{10}$$

$P_{y_{1/3}}$ and $P_{y_{2/3}}$ are the 33.3th and 66.6th percentiles of the distribution, respectively.

Member	Representative value		
Wall (S-G)	$R_{1,1} = 3.439$	$R_{1,2} = 3.599$	$R_{1,3} = 3.768$
Wall (G2)	$R_{2,1} = 3.937$	$R_{2,2} = 4.072$	$R_{2,3} = 4.211$

Table 2: Representative values of wall parameters.

Using the representative values of the parameters shown in **Table 2**, the numerical model M_k with parameter $\boldsymbol{\theta}_{\mathrm{k}}$ can be written as follows.

$$\begin{aligned} M_1 &= \{R_{1,1}, R_{2,1}\} \\ M_2 &= \{R_{1,1}, R_{2,2}\} \\ &\vdots \\ M_9 &= \{R_{1,3}, R_{2,3}\} \end{aligned} \tag{11}$$

Each model class is assumed equally likely, and the prior probability mass function of each model class $p(M_k|\mathcal{M})$ is assumed to take a discrete uniform.

3.3 Input ground motion

Table 3 shows the ground motion applied to the numerical model for seismic response analysis. The "Kokuji Wave" is simulated by fitting the acceleration spectra specified by the Building Standard Law in Japan.

In the limit strength calculation, there is a reduction factor that provides a correction for buildings with less than five stories. For a three-story building, the reduction factor is set to 0.9 [13]. Therefore, in this experiment, the seismic motion with a scaling factor of 90%, corresponds to large-scale earthquake ground motion in the Building Standard Law.

For each ground motion, the scaling factors is searched for when the maximum inter-story drift angle will become approximately 1/30 rad, with averaged model parameters. The search is initially conducted roughly in increments of 10% scale, and subsequently in increments of 1%.

Because it is demanding to immediately identify the exceedance of the threshold, 1/30 rad, and also because it is safer to misclassify the model to have risk slightly below the threshold, the scaling factor in which the maximum inter-story drift angle is between 1/30 × 0.9 rad and 1/30 rad will be excluded. When $F_{3/10}$ is the scaling factor in which the maximum inter-story drift angle is right before 1/30 × 0.9 rad, and $F_{1/30}$ is the scaling factor in which the maximum inter-story drift angle is right after 1/30 rad. 14 scaling factor is chosen for each "First Earthquake Motion" as follows.

- Seven scaling factors equally dividing from 0.5 to $F_{3/10}$.
- Seven scaling factors $F_{1/30}, F_{1/30} + 0.01, F_{1/30} + 0.02, F_{1/30} + 0.03, F_{1/30} + 0.1, F_{1/30} + 0.15$.

Each input ground motion was multiplied by a 14 scaling factors, and excited each of the 9 models.

	First Earthquake Motion	Second Earthquake Motion
Train data	2007 Chuetsu-oki earthquake record 2011 Tohoku earthquake record 2016 Kumamoto earthquake record (foreshock)	"Kokuji Wave" 90%
Test data	2016 Kumamoto earthquake record (main shock)	"Kokuji Wave" 90%
Small-scale earthquake ground motion for parameter updating	"Kokuji Wave" 50%	

Table 3: Input ground motions.

4 RESULTS

4.1 Bayesian updating

From Eqs. (1–4) Bayesian updating was conducted by comparing measured and simulated responses. 30 target model parameters were sampled from the lognormal distribution of the parameter using Latin hypercube sampling. The skeleton curve of the parameters is varied according to the value of the sampled data. "Kokuji Wave" factored by 50% was used as the small-scale earthquake. The matrix of the posterior distribution for the 30-target model is shown in **Fig. 5**.
The distribution was updated 3 times using the last 30 s of the measured data. Three channels of the acceleration sensors were observed at the second, third and roof floors ($N_o = 3$), with total of 1000 data ($N_t = 100$ Hz $\times$ 10 s $= 1000$) per step. In approximately half of the 30-target model, the update allowed the parameter to narrow down to a single numerical model M_k.

4.2 Neural network damage classifier (before update)

The number of elements in the training data input is 4 × 1 × 100 Hz × 1 s = 400. Thirty seconds of acceleration response was used for each ground motion. As it was difficult to classify from responses that were too small, data were considered invalid if the ground acceleration never exceeded 20 cm/s^2 in the data segment of 1 s.

The performance metrics used to evaluate the classification results were accuracy, precision, recall, and F1 score. F1 score represents the harmonic mean of the precision and recall. Each metric can be expressed using the confusion matrix notation in **Table 4**.

		Predicted label	
		1: Above 1/30 rad	0: Below 1/30 rad
True label	1: Above 1/30 rad	True positive (TP)	False negative (FN)
	0: Below 1/30 rad	False positive (FP)	True negative (TN)

Table 4: Confusion matrix.

$$\text{Accuracy} = \frac{TP + TN}{TP + FP + FN + TN} \tag{12}$$

$$\text{Precision} = \frac{TP}{TP + FP} \tag{13}$$

$$\text{Recall} = \frac{TP}{TP + FN} \tag{14}$$

$$\text{F1 Score} = 2 \times \frac{\text{Precision} \times \text{Recall}}{\text{Precision} + \text{Recall}} \tag{15}$$

Figure 6 shows graphs of accuracy and loss during the training. The training was ended at 100 epochs and NN weights with the highest validation accuracy were used for the NN model to classify the test data.

Figure 5: Joint probability of discrete random variables (30 model).

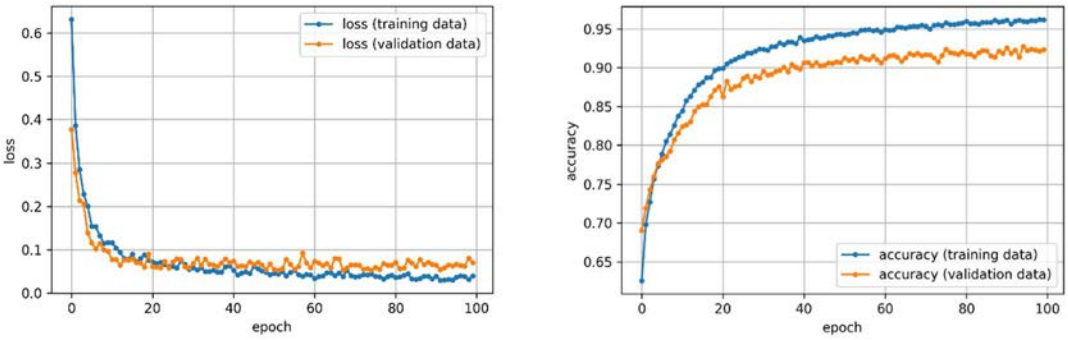

Figure 6: Accuracy and loss during the training.

The parameter of the computational model for the test data was varied using the same 30 target models in the Bayesian updating so that it could be compared with the NN classifier after the update.

As shown in **Table 5**, the accuracy for the test data was 73.8%. The other performance metrics were precision 59.3%, recall 89.1%, and F1 score 71.2%. The low precision shows that many safe buildings were misclassified as dangerous buildings.

		Predicted label		Total
		1: Above 1/30 rad	0: Below 1/30 rad	
True label	1: Above 1/30 rad	3167	384	3551
	0: Below 1/30 rad	2172	4027	6199
Total		5339	4411	9750
			Accuracy:	0.738

Table 5: Confusion matrix of test data.

4.3 Tuned neural network damage classifier (after update)

The NN damage classifier was trained using the weighted binary cross entropy loss function. Using Eq. (8), the values of posterior distribution shown in **Fig. 5** was used as the weight coefficient. Because there were 30 target models considered, the NN damage classifier was trained 30 times independently. The confusion matrix below shows the total amount of prediction in the 30 models.

		Predicted label		Total
		1: Above 1/30 rad	0: Below 1/30 rad	
True label	1: Above 1/30 rad	3329	222	3551
	0: Below 1/30 rad	700	5499	6199
Total		4029	5721	9750
			Accuracy:	0.905

Table 6: Confusion matrix.

The accuracy for the test data was 90.5% and other metrics were precision 82.6%, recall 93.7%, and F1 score 87.8%. The tuned NN damage classifier after the update reached 16.7 percentage points higher in accuracy than before the update.

5 CONCLUSIONS

A damage classifier for wooden structure was developed using NN to classify the risk of collapse in the next large earthquake that the building may experience. One of the challenges in predicting the seismic response of a wooden structure is that the effect of variance in its material and structural properties is relatively significant. To account for the uncertainty in the structural parameters, we propose a new method to update the damage classifier according to the parameters of the target building. The training data employed simulation results from seismic response analysis using a numerical model of a wooden structure. By using Bayesian updating with the measured data of a small- to medium-scale earthquake ground motions, which are more likely to occur before a major earthquake in the risk of collapse, we narrowed down the probability distribution of the structural parameters.

The proposed method uses the value of the posterior probability calculated by Bayesian updating as the weighting coefficient in the loss function of the NN, according to the data obtained from the target structure with the corresponding parameters. The method utilizes the weighted loss function to reflect the updated probability distribution of the structural parameters to the NN. By comparing the accuracy before and after updating the NN damage classifier, the tuned NN damage classifier achieved a higher accuracy. Future work should include confirmation of the proposed method using different target buildings from the present study and validation using response data from full-scale buildings.

REFERENCES

[1] National Institute for Land and Infrastructure Management, *Report of the Committee to Analyze the Causes of Building Damage in the Kumamoto Earthquake*, 2016. (in Japanese)

[2] S.T. Peterson, D.I. McLean, M.D. Symans, D.G. Pollock, W.F. Cofer, R.N. Emerson, and K.J. Fridley, Application of dynamic system identification to timber beams. *Journal of Structural Engineering*, **127**, 418–432, 2001.

[3] Y. Nakamura, A. Take, A. Mita, A study on damage evaluation method of wooden houses focusing on dynamic characteristics of output error. *Summaries of Technical Papers of Annual Meeting Architectural Institute of Japan*, **B-2**, 693–694, 2009. (in Japanese)

[4] M. Shiomitsu and Y. Sakai, A study on determination method of building damage degree from a single acceleration sensor attached to a building during a major earthquake (Part 3): Estimation of maximum deformation angle by elongation of period before and after earthquake using experimental data of full-size wooden building vibration. *Summaries of Technical Papers of Annual Meeting Architectural Institute of Japan*, **Structure II**, 1017–1018, 2010. (in Japanese)

[5] R. Tanida, R. Oiwa, T. Ito, and T. Kawahara, wooden framed house structural health monitoring by system identification and damage detection under dynamic motion with artificial intelligence sensor using a model of house including braces. *Proceedings of the 2018 IEEE International Conference on Computational Intelligence and Virtual Environments for Measurement Systems and Applications (CIVEMSA)*, Ottawa, ON, Canada, June 12-13, 2018, pp. 1–5.

[6] T. Saito, Evaluation of seismic response of buildings and probabilistic damage estimation applying Bayesian model updating. *Journal of Structural and Construction Engineering,* **78**, 61–70, 2013. (in Japanese)

[7] J.L. Beck, Bayesian system identification based on probability logic. *Structural Control and Health Monitoring*, **17**, 825–847, 2010.

[8] F. Gomez, Y. Narazaki, V. Hoskere, B.F. Spencer, and M.D. Smith, Bayesian inference of dense structural response using vision-based measurements. *Engineering Structures*, **256**, 113970, 2022.

[9] N. Levine, T. Golecki, F. Gomez, B. Eick, and B.F. Spencer, Bayesian model updating of concrete-embedded miter gate anchorages and implications for design. *Structural and Multidisciplinary Optimization*, **66**, 60, 2023.

[10] T. Yamashita, M. Kohiyama, and K. Watanabe, Deep neural network for detecting earthquake damage to brace members installed in a steel frame. *Japan Architectural Review*, **4**, 56–64, 2021.

[11] National Research Institute for Earth Science and Disaster Resilience: ASEBI: Archives of E-Defense Shakingtable Experimentation Database and Information. https://doi.org/10.17598/nied.0020

[12] T. Nakagawa, M. Ohta, T. Tsuchimoto, and N. Kawai, Collapsing process simulations of timber structures under dynamic loading III: Numerical simulations of the real size wooden houses. *Journal of Wood Science*, **56**, 284–292, 2010.

[13] Ministry of Land, Infrastructure, Transport and Tourism, Housing Bureau, Building Guidance Division, *2001 Edition of Limit Strength Calculation Method Calculation Examples and Commentary*, 2006. (in Japanese)